Materials Science & Engineering A 631 (2015) 10–17

Contents lists available at ScienceDirect

Materials Science & Engineering A

journal homepage: www.elsevier.com/locate/msea

Comparison of dislocation density based approaches for prediction of defect structure evolution in aluminium and copper processed by ECAP

V. Bratov [a,b,*], E.N. Borodin [b,c]

[a] Saint-Petersburg State University, Saint-Petersburg, Russia
[b] IPME RAS, Saint-Petersburg, Russia
[c] Chelyabinsk State University, Chelyabinsk, Russia

ARTICLE INFO

Article history:
Received 28 November 2014
Received in revised form
27 January 2015
Accepted 10 February 2015
Available online 21 February 2015

Keywords:
ECAP
Modelling
Dislocation density
DRX
FEM

ABSTRACT

Three known dislocation density based models are compared to each other, and to available experimental results. All three models were embedded into ANSYS finite element (FE) software and firstly utilised to predict aluminium and copper transformations (dislocation density evolution and the resulting grain size) in a result of a single pass of equal channel angular pressing (ECAP). It is demonstrated that for the studied problem dislocation density evolution under severe plastic deformation (SPD) can be precisely predicted utilizing simple classical model. One of the models was utilized to predict defect structure evolution for the series of ECAP passes. Simulations have revealed that within the framework of the proposed model the increase of the dislocation density on ECAP pass is proportional to yield strength increment on the previous pass for both studied materials. This fact gives grounds to a proposal of a semi-analytical approach, predicting dislocation density evolution in a result of consequent ECAP passes on the basis of a numerical simulation of the two first passes. The utilized kinetic model for dislocation density evolution separates between densities of mobile and immobile dislocations. Employing the idea of separation of dislocations into mobile and immobile, a new approach for dynamic recrystallization coupling dislocation density and the size of grain formed in metal is proposed. The proposed approach for dynamic recrystallization appeared to be applicable for the whole range of grain sizes.

1. Introduction

Severe plastic deformation (SPD) technologies for metal processing are being intensively developed during several recent decades [1–5], but only in the last years these technologies approached the level of practical application on industrial scale [5]. The essence of these technologies consists in considerable refinement of characteristic size of material defect structure in the process of plastic deformation. For many materials it is possible to reduce the predominant grain size by several orders of magnitude, which can often give unique mechanical properties to the processed material [1,5]. A mathematical simulation of these processes is substantial for understanding of structural transformations within material during deformation and for predictions of optimal technological process parameters (including process geometry, rate, etc.). At the same time an overwhelming majority of simulations is performed on the basis of phenomenological models, not accounting material structure evolution. This kind of modelling cannot provide a wide range of possibilities for prediction of material behaviour – in most cases significant changes in experimental conditions (geometry, rate, etc.) would require a new experimental evaluation of parameters needed for modelling or even model modification in order to fit the observed experimental results. Obviously these kinds of models are not applicable in order to optimize technological parameters for SPD material modification processes. Nor are these models principally able to provide information about defect structure of a deformed material, distribution of defects within the material or estimate minimum possible grain size for given experimental conditions. The result of the unmet need of adequate modelling with effective prediction ability is that SPD technologies development is nowadays mainly based on extensive experimental work being extremely resource consumptive and rather ineffective.

Nowadays none of the known models can offer a correct prediction of deformation that should be applied to a sample in order to receive desired defect structure with a-priori given physical properties. At the same time the available dislocation based plasticity models [6–10] are able to make a reliable prediction of resultant material grain size after one or several ECAP passes [10]. Unfortunately these models contain several “trimming” parameters that should be

* Corresponding author. Tel.: +7 812 321 47 79; fax: +7 812 321 47 74.
E-mail addresses: vladimir@bratov.com (V. Bratov), elbor7@gmail.com (E.N. Borodin).

http://dx.doi.org/10.1016/j.msea.2015.02.019
0921-5093/

evaluated experimentally. For instance measured data from metallic samples after different number of ECAP passes can be used to evaluate these parameters [11]. Further development of ultrafine-grained (UFG) structure material engineering requires an analysis of the existing models of SPD, a study of influence of "trimming" parameters on the received solutions, a study of the possibility to provide clear physical meaning and measurability to these parameters, a study of validity limit of these models, etc. The final result should consist in appearance of a rather universal material behaviour model having no "trimming" parameters and applicable for prediction of a wide range of processes and materials.

This work is an attempt to analyse three known dislocation density based plasticity models and study their applicability and distinctive features providing a possibility to predict different peculiar properties of material defect structure evolution under SPD of metals. Embedment of these models into FE computational schemes will give a possibility to assess differences in the results, compare received defect distributions to available experimental data and draw inferences considering necessity to modify the classical metal dislocation plasticity model with additional features.

2. Dislocation density based plasticity models

Several approaches utilizing local dislocation density as the main characteristic for metal plastic deformation are known [6–10]. Central quantity defining number of dislocations in crystal is the scalar dislocation density – total dislocation length per unit volume. Knowledge of distribution of scalar dislocation density within material gives a possibility to estimate size of grains formed as a result of ECAP and provides detailed information about static yield strength of the material. All of the concerned kinetic models contain dislocation sources, allowing for possibility of dislocation nucleation on dislocation forest or inclusion atoms and dislocation drains accounting for annihilation of dislocation pairs. Usage of semi-empirical parameters in these models gives a possibility to predict the most important processes within the dislocation ensemble without a concrete definition of variety of these complex processes.

2.1. A classical model

Within the framework of the classical model scalar dislocation density ρ_D as a function of strain ε is given by [6,8]

$$\rho_D'(\varepsilon) = C + A\sqrt{\rho_D(\varepsilon)} - B\rho_D(\varepsilon), \tag{1}$$

where the first two terms $C \sim \delta_0\sigma_y^0/Gb^2$ and $A \sim \delta_f/b$ are responsible for dislocation density growth as a result of nucleation on dislocation forest and inclusions and the last term $B = k_a$ stands for annihilation of the dislocation pairs. Here G is the material shear modulus, b is the Burgers vector, σ_y^0 is the yielding limiting stress for a dislocation free annealed material. Model parameters δ_0,δ_f and k_a are, in essence, trimming parameters that should be evaluated empirically.

An important property of (1) (while $C = 0$), is the existence of the maximum possible dislocation density $\rho_D^{\max} = (\delta_f/bk_a)^2$, thus (1) can be rewritten as

$$\frac{d\rho_D}{d\varepsilon} = \frac{\delta_0}{Gb^2}\sigma_y^0 + k_a\rho_D\left(\sqrt{\frac{\rho_D^{\max}}{\rho_D}} - 1\right), \tag{2}$$

According to [6] k_a obtains values between 2 and 9 for the majority of metallic materials. Fig. 1 presents calculated dislocation densities for deformed aluminium as a function of strain for different values of k_a whilst $\delta_f = 0.01$ and $\delta_0 = 0.02$ [6]. The dots denote experimentally measured dislocation densities in the boundaries of dislocation substructure cells received after a varied number of ECAP passes of aluminium [11]. It was found that the best coincidence of classical model approximation with the experiment is achieved for $k_a \sim 4.5$.

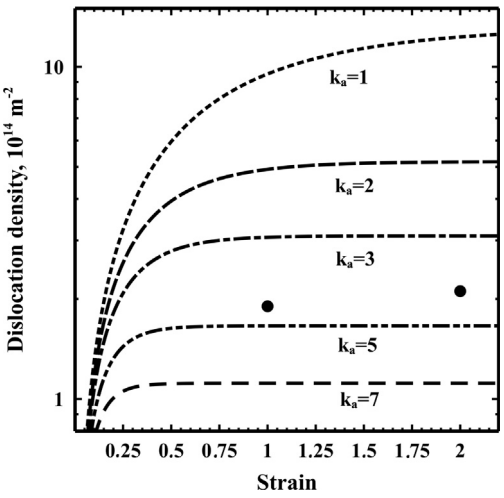

Fig. 1. Dislocation density as a function of strain for different values of annihilation coefficient. The dots correspond to the experimental data from [11].

2.2. Modification of the classical model for a separate account of mobile and immobile dislocation densities

A model proposed by Mayer and co-authors [7,8,12] extends the applicability limits and improves the classical model. Originally this model was proposed having in mind a possibility to model plasticity at high strain rate deformation. For quasistatic case it can be reduced to a classical model with the principal distinction from the model (1) consisting in separation of dislocation density ρ_D into two parts giving densities for mobile ρ_D^{mob} and immobile ρ_D^{im} dislocations. Evolution of dislocation densities is given by the following kinetic equations [7]:

$$\begin{aligned}\frac{d\rho_D^{mob}}{dt} &= k_g b^2\sigma_y|V_D|\rho_D^{mob} - V_C\left(\rho_D^{mob} - \rho_D^0\right)\sqrt{\rho_D^{im}} - k_a b|V_D|\rho_D^{mob} \\ &\quad\times\left(2\rho_D^{mob} + \rho_D^{im}\right) \\ \frac{\rho_D^{im}}{dt} &= V_C\left(\rho_D^{mob} - \rho_D^0\right)\sqrt{\rho_D^{im}} - k_a b|V_D|\rho_D^{mob}\rho_D^{im}.\end{aligned} \tag{3}$$

here $k_g = \eta/\varepsilon_L b$ is the coefficient responsible for dislocation generation. Using the Orowan equation for plastic strain rate [9] $\dot\varepsilon_{plast} = \rho_D^{mob} b|V_D|$, (3) can be rewritten as

$$\begin{aligned}\frac{d\rho_D^{mob}}{d\varepsilon} &= \left(k_g b\sigma_y^0 + \alpha Gb^2 k_g\sqrt{\rho_D^{im} + \rho_D^{mob}}\right) - \frac{V_C\left(\rho_D^{mob} - \rho_D^0\right)\sqrt{\rho_D^{im}}}{\dot\varepsilon_{pl}} \\ &\quad - k_\alpha^m\left(2\rho_D^{mob} + \rho_D^{im}\right) \\ \frac{\rho_D^{im}}{d\varepsilon} &= \frac{V_C\left(\rho_D^{mob} - \rho_D^0\right)\sqrt{\rho_D^{im}}}{\dot\varepsilon_{pl}} - k_\alpha^i\rho_D^{im}\end{aligned} \tag{4}$$

If the hardening rate is small, plastic flow within calculation time step can be considered as a steady state flow and $\dot\varepsilon_{plast} = \dot\varepsilon$. Besides that in [8] it is considered that parameters for the model (1) can be presented as $\delta_f = \alpha\eta Gb^3/\varepsilon_L$, $\delta_0 = \delta_f\alpha^{-1}$, where $\alpha \sim 0.5$ is the Taylor constant [6,7], $\varepsilon_L = 8eV/b$ is the elastic energy of dislocation length unit [7,13], $\eta \sim 0.1$ is the fraction of work of plastic deformation stored in the form of defects. By various estimates [13,14] for small strains this value should be around 10%. For higher strains the value of η becomes several times less [14]. Using these parameters it is possible to receive estimations for the classical model parameters [13] $\delta_f \sim 0.01$ and $\delta_0 \sim 0.02$. These values are normally utilized for the classical model based

simulations [6]. Thus, the model [7,8] adds two new parameters to the ones used within the classical model [6]: the rate of dislocation immobilization V_C and the annihilation constant for immobile dislocations k_α^i. The computations show that the value of k_α^i is close to the value of k_α^m – the annihilation constant for mobile dislocations. With the increase of the immobilization rate V_C, dislocation density for immobile dislocation is monotonously growing, while the density for mobile dislocation is decreasing. Evolution of mobile dislocation density is not monotonous with the strain increase. For large values of immobilization constant, density reaches its maximum value for a definite strain value, decreasing to stationary level with the following strain increase. This kinetic behaviour of mobile dislocation is adequate to experimental measurements of dislocation density in the centre of dislocation cells. [15,16]. The experimental data [11] should correspond to the dislocation density of immobile dislocations.

Fig. 2 presents the scalar density for mobile and immobile dislocations as a function of immobilization rate for strain equal to 2. The maximum dislocation density is reached at the intersection point. Both densities are stabilized for high and low values of V_C reaching the level corresponding to the maximum dislocation density ρ_D^{max}.

Numerical simulation of ECAP process using dislocation density based models will require a set of model parameters. Obviously these parameters should be chosen from the requirement of correspondence to some of the known experimental data. Fig. 3 compares the classical (1) and the mobile/immobile dislocation (4) models to the experimental results [11] and [17]. The same figure gives densities of mobile and immobile dislocations as a function of strain. As follows from Fig. 3, both models can provide a good coincidence with the experimental measurements. This result stands for applicability of the classical model to predict aluminium hardening as the strain is increasing. At the same time the model (4) can give a more detailed insight into the evolution of metal defect structure by separation between mobile and immobile dislocations. This result can obtain an extreme significance for the processes where the number of mobile dislocations is of critical importance.

The following values of the model parameters were used to compute data introduced in Fig. 4: $k_a = 5.7$, $k_\alpha^i = 7$, $k_\alpha^m = 4$, $\delta_0 = 0.02$, $\eta = 0.1$, $\varepsilon_L/b = 8$ eV, $V_C = 2.5 \times 10^{-6}$ m/s, $\rho_D^0 = 10^{13}$ m^{-2}, $\rho_D^{mob} = 10^{13}$ m^{-2}, $\rho_D^{im} = 10^{14}$ m^{-2}.

2.3. Model considering evolution of dislocation sub-boundaries in the process of deformation

Another approach to dislocation density evolution kinetics was proposed by Estrin with co-authors [9,10]. The essential difference of this model from the models described above (1,4), consists in

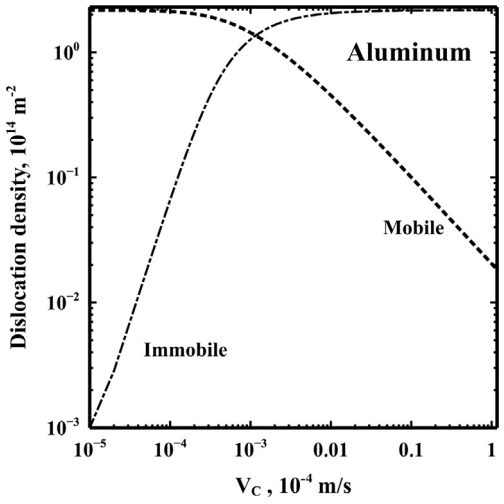

Fig. 2. Immobile and mobile dislocation density as a function of immobilization rate.

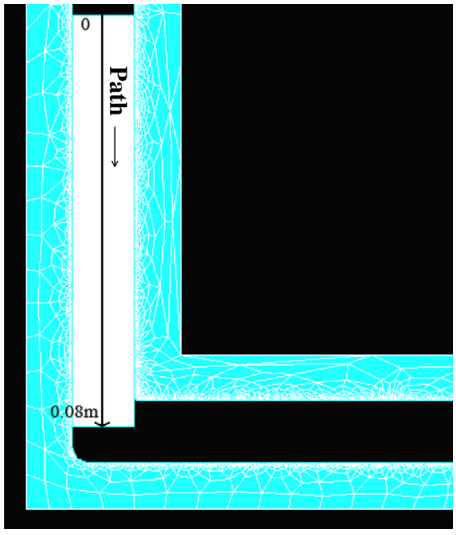

Fig. 4. Path for data presented on graphs.

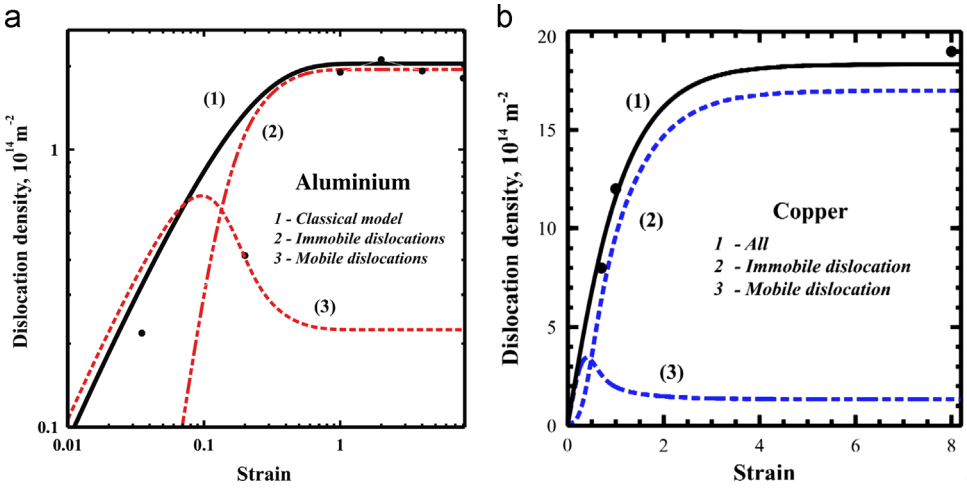

Fig. 3. Dislocation density as a function of strain for the classical [6] (1) and the mobile (3)/immobile (2) [7] dislocation models. The dots stand for the experimental data from [11] for aluminium and from [17] for copper.

model enhancement with a new rule predicting evolution of cell walls and dislocations forming these walls. The proposed rule [9] is empiric and introduces a number of additional parameters into the model. The following equations are written for the evolution of densities of dislocations in cells and dislocations within cell walls [9,10]:

$$\frac{d\rho_D^{cell}}{dt}=\alpha^*\frac{1}{\sqrt{3}}\frac{\sqrt{\rho_D^{wall}}}{b}\dot{\gamma}^{wall}-\beta^*\frac{6}{bd(1-f)^{1/3}}\dot{\gamma}^{cell}-k_0\left(\frac{\dot{\gamma}^{cell}}{\dot{\gamma}_0}\right)^{-1/n}\dot{\gamma}^{cell}\rho_D^{cell}$$

$$\frac{d\rho_D^{wall}}{dt}=\frac{6\beta^*(1-f)^{2/3}}{bdf}\dot{\gamma}^{cell}+\frac{\sqrt{3}\beta^*(1-f)\sqrt{\rho_D^{wall}}}{fb}\dot{\gamma}^{cell}-k_0\left(\frac{\dot{\gamma}^{wall}}{\dot{\gamma}_0}\right)^{-1/n}\dot{\gamma}^{wall}\rho_D^{wall} \quad (5)$$

Supposing that $\dot{\gamma}^{wall}=\dot{\gamma}^{cell}=\dot{\varepsilon}_{pl}$ and assuming that $\dot{\gamma}_0=1$, according to [18] dislocation density increment as a result of strain alternation (5) can be rewritten as

$$\frac{d\rho_D^{cell}}{d\varepsilon}=\frac{\alpha^*\sqrt{\rho_D^{wall}}}{\sqrt{3}b}-\frac{6\beta^*}{bd(1-f)^{1/3}}-k_0\left(\dot{\varepsilon}_{pl}\right)^{-1/n}\rho_D^{cell}$$

$$\frac{d\rho_D^{wall}}{d\varepsilon}=\frac{6\beta^*(1-f)^{2/3}}{bdf}+\frac{\sqrt{3}\beta^*(1-f)\sqrt{\rho_D^{wall}}}{fb}-k_0\left(\dot{\varepsilon}_{pl}\right)^{-1/n}\rho_D^{wall} \quad (6)$$

It can be seen that by the form (6) is analogues to the classical model (1) with slightly modified terms for dislocation nucleation and annihilation rates. It can also be seen that the models (4) and (6) have a similar structure predicting immobilization (migration to cell walls) of mobile (cell) dislocations with increasing strain. In contrast to the model (4), the model (6) is introducing an additional source of immobile (cell wall) dislocations – new dislocation loops can appear within the walls of dislocation cells among stationary "dislocation forest". A new parameter here is the cell walls fraction volume that is changed with the change of the equivalent plastic strain following an empiric law:

$$f=f_{\inf}+(f_0-f_{\inf})\exp(-\varepsilon_{pl}/\tilde{\gamma}). \quad (7)$$

Obviously the average dislocation density over the volume unity should be calculated as

$$\rho_D=f\rho_D^{im}+(1-f)\rho_D^{mob}. \quad (8)$$

Simulations utilizing this model presented later in this paper use the following model parameters [10]: $f_0=0.25$, $f_{\inf}=0.06$, $m=100$, $n=67$, $\tilde{\gamma}=3.2$, $\alpha^*=0.0024$, $\beta^*=0.0054$, $k_0=3.22$.

Here one can conclude that the three models have a common basis (the classic model) and enrich each other. Additional complications of the classical model increase the number of kinetic parameters that should be evaluated empirically (i.e. by fitting). Obviously introduction of additional parameters would increase model flexibility. At the same time model universality can be significantly reduced – a possibility to perform modelling for a wide range of processes using a single set of model parameters vanishes. Besides that, evaluation of additional model parameters requires additional experimental data to be used for parameter identification. The following sections of the paper discuss the requirements to dislocation kinetics model, that are essential for an accurate numerical simulation of evolution of defect structure of metals processed by ECAP, taking into consideration the accuracy of experimental data available at the moment.

3. FEM modelling of ECAP process

All the three models for dislocation density evolution were embedded into a computational code based on Finite Element Method (FEM). New plasticity models were implemented as USERMAT FORTRAN subroutine for ANSYS commercial finite element software. The subroutine is executed during element results calculation and provides a possibility to update local dislocation densities in every point of the deformed sample. Dislocation densities are updated every time integration substep according to the local material deformed state in compliance with equations corresponding to the model used (1 or 4 or 6).

Since a static problem is solved, time integration is not performed. The problem is formulated as a number of consequent static substeps given by displacement gradually applied to the top of the deformed bar. Time is eliminated from state equations. Stresses and strains in the deformed bar on each substep are calculated according to elastic deformation model. Once a stress at some point of the bar reaches the value outside von Mises plastic flow surface, plastic flow is onset at this point. The strain that appeared at that point due to displacement applied at the top of the bar is split into elastic and plastic parts, returning the stress to the plastic flow surface. Alteration of plastic part of strain tensor is affecting dislocation densities according to (1 or 4 or 6). Thus, dislocation density alteration is always executed at a flow stress that is altered if dislocation density is changed. In other words, plastic flow is resulting in dislocation density alteration that, for its turn, is updating the flow stress and the flow surface.

The same subroutine updates local yield stress at every point of the sample once it should be changed due to the local dislocation density change. Material yield limit has the meaning of barrier stress that should be exceeded in order to initiate dislocation sliding. The change of the yield stress in the process of deformation can be predicted using the Taylor law and the Hall–Petch empirical relationship [19]:

$$\sigma_y=\sigma_0+\alpha Gb\sqrt{\rho_D}+k_{HP}/\sqrt{d} \quad (9)$$

Obviously, the grain structure that is formed after ECAP pass should affect deformation of the material during the next ECAP pass. Once the local yield stress is changed the subroutine starts using new local material parameters to calculate stresses and elastic/plastic strains in the point according to von Mises yielding model.

Simulation results provided for analysis include sample shape for all simulation substeps along with the history of all state variables for all the sample points. Controlled state variables include stresses, elastic/plastic strains, dislocation density (densities of cell/cell walls dislocations for the model (6) or mobile/immobile dislocations for the model (4), etc. After simulation completion new grain size can be calculated for all the sample points from dislocation density. ECAP process for aluminium grain refinement was modelled utilizing the developed FEM model. In order to optimize the computational time 2D plane strain conditions were supposed. Experimental geometry was chosen to comply with the experiments [11] (Fig. 4).

Initial material properties were taken from Table 1.

The utilized model parameters are given in Section 2.2 for the models (1) and (4) and in Section 2.3 for the model (6). At this stage a single ECAP pass was simulated. Identical simulation conditions (geometry, initial material properties, etc.) were used for all the three models.

The results for equivalent strain distribution after a single ECAP pass are presented in Fig. 5. Equivalent strain distribution as a

Table 1
Utilized material parameters for aluminum and copper.

Material	G (GPa)	b (nm)	σ_y^0 (MPa)	α	k_{HP} (MPa$\sqrt{\text{mm}}$)
Aluminum	26.3	0.286	70	0.25	2.5
Copper	42	0.256	150	0.25	3.5

function of distance along initial sample vertical symmetry line (see path in Fig. 4) is almost identical for the models (1) and (4) while the results for the model (6) are slightly different.

Fig. 6 introduces a calculated distribution of total dislocation density for the models (4) and (6). Fig. 7 gives the same value along the path given in Fig. 4. Results for the model (1) are qualitatively very close to predictions given by the model (4). As seen in Fig. 6, in coincidence with numerous ECAP experiments, the down-right corner of the initial sample in the process of deformation becomes the front-down corner of the deformed sample, whilst the down-left corner of the initial sample forms a stress concentrator on the down surface of the processed sample.

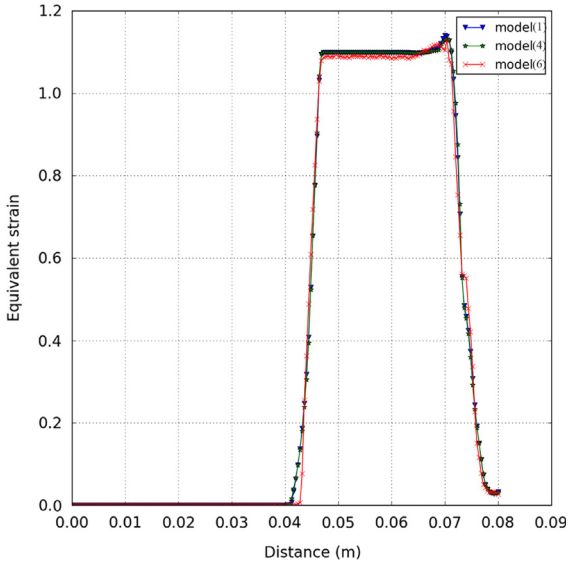

Fig. 5. Distribution of equivalent strain in aluminium bars processed by ECAP.

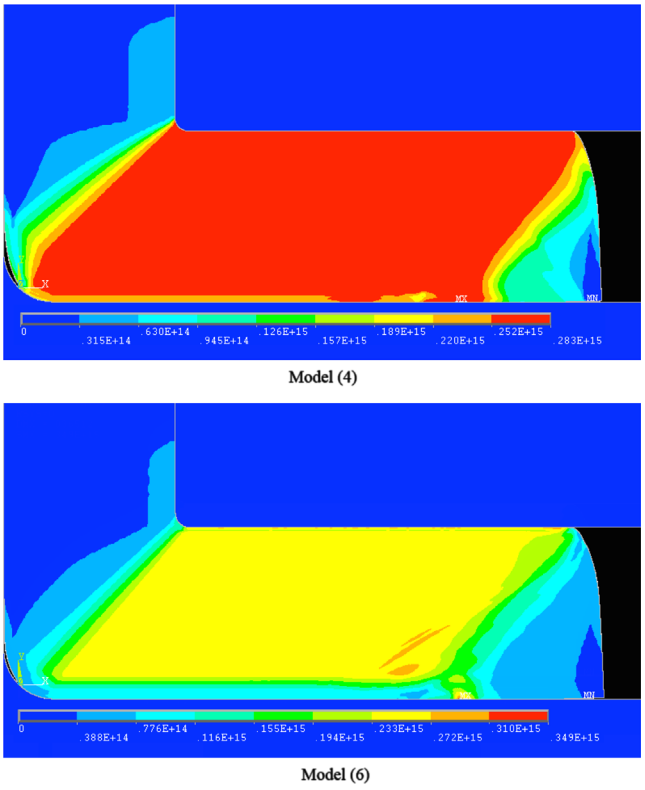

Fig. 6. Distribution of total dislocation density.

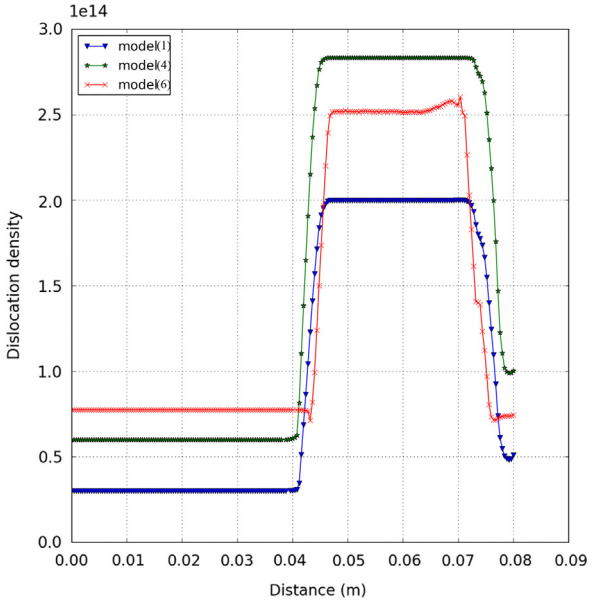

Fig. 7. Distribution of total dislocation density.

As previously, the models (1) and (4) demonstrate a similar behaviour whilst the model (6) displays slight differences in dislocation density distribution. The received dislocation densities after the first ECAP pass are very close (2.10^{14}–$2.8.10^{14}$ m^{-2}) and comparable to the experimentally measured value of grain size [10] after a single ECAP pass calculated using $d = \beta \rho_D^{-1/2}$ [10] with $\beta = 20$. As follows from the presented figures, sharp increase of the dislocation density is achieved in a small area adjacent to the form angle (*5* mm of the path length). Nonuniform distribution of dislocation density characterizes the front end zone of the deformed bar. The length of this zone is of the order of the bar cross sections (*1–1.5* cm) and is the largest in predictions given by the model (6). Original front surface of the bar is deformed to slide along the bottom of the form. Distribution of dislocation density within the bulk of the material is uniform, not accounting for the thin layer adjacent to the bottom of the form.

Similar results were received while modelling ECAP of copper. The three analysed models, in analogue to aluminium results, give similar predictions showing distribution of dislocation densities in the bulk of the material that is close to homogeneous. A general conclusion for this section is that for single ECAP pass computational results obtained by each of the three models are close to the available experimental data. Predictions given by the model (1) and the model (4) are very similar whilst the model (6) is showing a slight distinction. Hence, if the dislocation density evolution at ECAP process is the only aim of the simulation, a simple kinetic model without additional fitted parameters may be used.

4. Several ECAP passes for aluminium and copper

Utilizing the developed approach it is also possible to predict modification of material in a result of several consequent ECAP passes. Here the model (4) will be used to predict formation of fine grain structure in copper and aluminium, which can be compared to the available experimental results. Within the framework of the model, dislocation density is supposed to be the main characteristic that controls the process of SPD. In the process of deformation yield limit is continuously updated in every point of the processed material as a result of local dislocation density change. The connection between the yield stress and the local dislocation density is supposed to be given by the Taylor hardening law

[19,20]. It is supposed that after every ECAP pass dislocation density is reduced to its initial value whilst the dislocation spillover is utilized to create new grain boundaries according to dynamic recrystallization (DRX) model [10,21]. Obviously, the decrease of the material grain size is affecting the initial (for the next ECAP pass) material yield strength that is updated according to the Hall–Petch relation [20]. The increase of the initial yield stress for the next ECAP pass is resulting in higher flow stresses in the material, giving higher dislocation densities in the end of the next ECAP pass. Thus, modelling the consequent ECAP passes leads to consequent refinement of the material grain structure.

For practical purpose the most important result of numerical modelling can consist in prediction of resultant grain size as a function of accumulated strain or a number of ECAP pass. The model (4) being implemented into FEM computational scheme displays linear dependence of the received dislocation density in the bulk of the processed material on initial (for ECAP pass) material yield limit for both aluminium and copper. Fig. 8 demonstrates calculation result of mean dislocation density at the sample after an ECAP pass with a different initial yield strength value. In this model alteration of initial yield strength corresponds to simulation of different number of ECAP pass for initial coarse-grained aluminium and copper samples.

One can see from Fig. 8 that the increase of the dislocation density in material bulk as a result of the next ECAP pass is proportional to the increase of material yield limit in the result of the previous ECAP pass:

$$\Delta\rho_D^{(n+1)} = \lambda\,\Delta\sigma_y^{(n)}. \tag{10}$$

Numerical simulations give proportionality coefficients equal to $\lambda_{AL} = 3\times10^6\ \mathrm{m}^{-2}/\mathrm{Pa}$ for aluminium and $\lambda_{CU} = 1.2\times10^7\ \mathrm{m}^{-2}/\mathrm{Pa}$ for copper.

Dislocation density and grain size can be coupled once an assumption about dynamic recrystallization (DRX), taking place in a material undergoing SPD as the main mechanism of metal grain refinement, is made [20,21]. Dynamic recrystallization is the result of dislocation substructure evolution. The size of dislocation cells can be estimated from energetic reasoning [21]. If one compares energy of a group of dislocations homogeneously distributed in a unity of volume and the energy of dislocations (per unit volume) within the walls of dislocation cells [20], it can be found that above some definite dislocation density, it is energetically favourable to form dislocation cells, rather than maintain homogeneous distribution of dislocations. Searching for equality of energies of homogeneous distribution and the cell dislocation structure, critical dislocation density leading to cell formation can be found [21] $\rho_D^* = (3e/8d)^2$, here $e\sim2.71$. Thus, dislocation cell diameter as a function of dislocation density can be received as

$$d = \beta\rho_D^{-1/2}. \tag{11}$$

Here β is a coefficient of the order of 1 and dependent on dislocation cell geometry. It can be shown [21], that for elliptical cells $\beta=1$ and for spherical cells $\beta=2.6$. Eventually boundaries with small misorientation angles between adjacent cells evolve into large-angle grain boundaries with essentially disordered structure. Thus, it can be expected that (11) should give a mean value for a size of grain appearing in material after intensive plastic deformation. The problem is that the presented model of recrystallization is correct for equilibrium processes, which is not true for SDP processes. In [22,23] this approach was utilized to predict dynamic recrystallization and it was shown that in order to receive satisfactory coincidence with experimental data for sub-micrometre grain sizes, values for β between 10 and 30 should be used.

Substitution of (10) into DRX model (11), differentiation and accounting for Hall–Petch law [19] gives a recurrent formula that can be used to calculate grain refinement ratio in a result of any ECAP pass:

$$\Delta d_{n+1}/\Delta d_n = \frac{\lambda K_{HP} d_n^{3/2}}{4\beta^2} \tag{12}$$

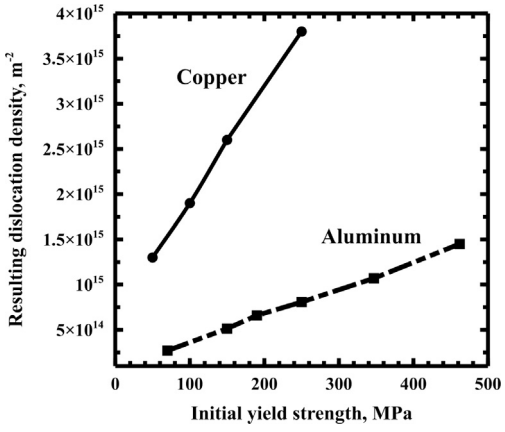

Fig. 8. Linear dependency between the initial yield limit (defined by the initial grain size via Hall–Petch relation) and the dislocation density formed in the bulk of the material after the next ECAP pass.

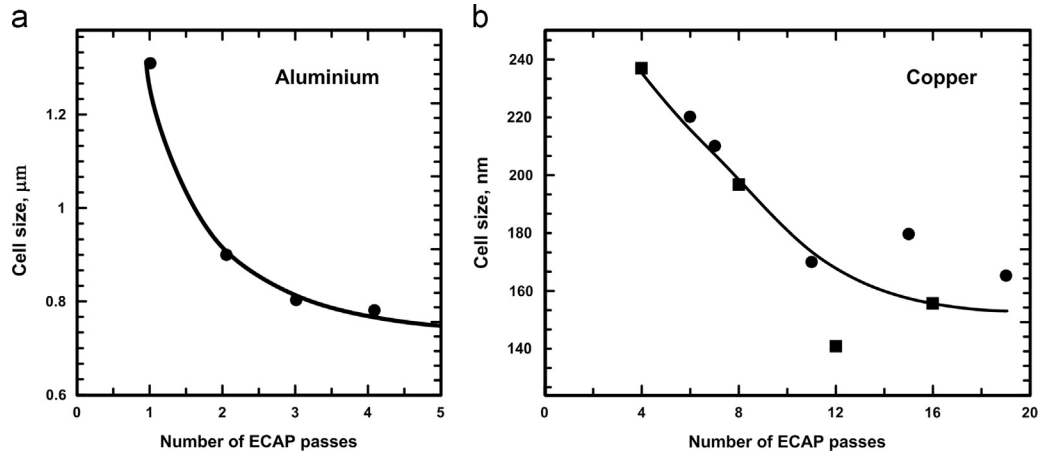

Fig. 9. Predictions of resultant grain size for ECAP process. Circles on figure (a) correspond to experimental data from [10] for aluminium. Squares on figure (b) correspond to experiments from [24] and circles to data from [23] for copper. Data from [23] is shifted to correspond to the grain size. Solid curves are calculated using (4) and (13).

Resultant grain size after arbitrary ECAP pass can be calculated as

$$d_N = d_0 + \Delta d_1 \cdot \sum_{k=1}^{N} \left(C^k \prod_{l=1}^{k} d_l^{3/2} \right), \tag{13}$$

where $C = \lambda K_{HP}/4\beta^2$, d_0 is the initial grain size and Δd_1 is the grain refinement in the result of the first ECAP pass.

Probably the linear dependency of the received dislocation density on initial (for the ECAP pass) material yield limit is the property of the utilized model and will hold for the arbitrary material. In order to evaluate Δd_1 and λ it is necessary to simulate the first two ECAP passes. After this (13) can be used to calculate resultant grain sizes as a function of ECAP pass number. Received dependencies for aluminium and copper are compared to the available experimental results in Fig. 9. As follows from the presented figures, numerical computations are in an excellent coincidence with the available experimental measurements.

The presented results stand for applicability of the developed model (4),(13) to predict experimentally received grain sizes as a result of ECAP process for aluminium and copper if the initial grain size is within submicrometre range. It is important that this approach utilizes just two adjustable parameters – significantly less as comparing to the majority of other known models (see Table 1 in [10]). At the same time it is observed that DRX model (11) is hardly applicable to predict recrystallization in the whole range of grain sizes.

Obviously the problem is connected to a certain inaccuracy and roughness of the utilized DRX model that needs to be corrected. Constant C in (13) contains squared dynamic recrystallization constant β in denominator. As a result, even a small change of the value for β will result in a significant impact on the value of C. Thus, the requirement on the precision of dislocation kinetics model is significantly reduced and can be easily fulfilled by the classical model (2) or its modification (4). Staying within the framework of DRX model (11) additional improvements of model of dislocation evolution are ineffective and will not result in additional accuracy of predictions of resultant grain size.

As already mentioned, this model, as well as (11), is only applicable for prediction of recrystallization in materials with submicrometre grain sizes, giving big discrepancies with experimental data for metals with bigger grain structure. In other words, this approach does not give a possibility to predict evolution of grain structure from large grains to ultra fine grains (UFG) under ECAP. Due to this reason, in [23] authors introduce a dependency for β:

$$\beta = \beta_\infty + (\beta_0 - \beta_\infty) \cdot \exp(-\gamma\varepsilon), \tag{14}$$

which results in appearance of three additional fitting parameters ($\beta_\infty = 57$ $\beta_0 = 112.56$ $\gamma = 0.2656$ for copper). Introduction of three adjustable parameters controlling β provides a possibility to fit experimentally observed grain size distribution (see eg. Fig. 10).

An alternative approach can be proposed should one suppose the degree of defect structure nonequilibrium to be an important factor controlling the process of dynamic recrystallization. This nonequilibrium state can be quantitatively measured by the flow of dislocations to cell boundaries and the dislocation immobilization rate. In order to do so, separation of dislocations into mobile and immobile, introduced in the model (4) can be employed. An example of such a reasoning can be found in [25], where authors grounded on the model (6) introduce new dislocation source explicitly accounting “immobilization probability” and “the flux of dislocations» to cell walls.

Suppose that the grain boundary structure is continuously evolving in compliance with “equilibrium” Eq. (11). It is known that the evolution of dislocation cell structure is not reflecting the evolution of grain structure and these processes can coexist. Suppose that the main event forming the future grain structure is the creation and consolidation of triple junctions of dislocation cell boundaries. Probability of such an event is supposed to be proportional to dislocation flow to cell boundaries. If one supposes that during this process a part of the elements of the future grain structure is consequently consolidated with time, then every definite level of a plastic strain corresponds to a definite size scale, larger than the size of dislocation cells given by Eq. (11). This size scale corresponds to the mean distance between consolidated elements (triple junctions) of the future grain structure. Should one introduce volume fraction of consolidated triple junctions J, then the mean distance between the elements of stable structure will be given by

$$d = \frac{\beta}{J}\rho_D^{-1/2}. \tag{15}$$

Obviously this distance exceeds the size of dislocation cells by the orders of magnitude. Utilizing the experimental data [26] and supposing, for simplicity, that the rate of nonequilibrium grain boundaries fraction change is proportional to the ratio between mobile to immobile dislocations, the following form of recrystallization law can

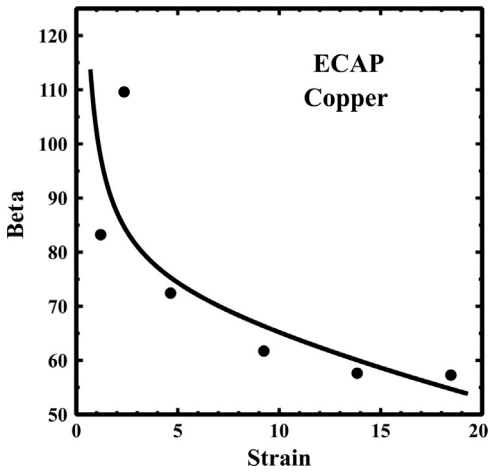

Fig. 10. The circles represent values of coefficient β calculated in [23] from condition of coincidence of resultant grain size with available experimental data. Solid line gives prediction using (16).

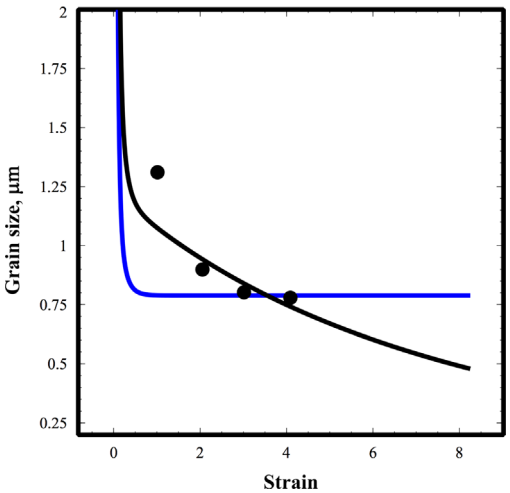

Fig. 11. The black line corresponds to calculation by (16) with $\beta = 2.6$. The blue line corresponds to calculation by (13) with $\beta = 21$. The circles correspond to the experimental data from [23].

be proposed:

$$\begin{cases} J = p^3 \\ \dot{p} = \alpha\left[V_C(\rho_D^{mob} - \rho_D^0)/\rho_D^{im}\right] \end{cases}, \quad (16)$$

where parameter p is the fraction of nonequilibrium boundaries of dislocation cells in dislocation structure. Fig. 10 presents a comparison between predictions given by (16) and values of parameter β evaluated in [23] from condition of coincidence of resultant grain size with the available experimental data.

Calculations show that in the model (16) the annihilation coefficient is significantly affecting $\beta(\varepsilon)$ for large strains. The approach is shown to be applicable to predict experimentally observed correlation between the accumulated strain and the observed resultant grain size (see Fig. 11). The best coincidence between the studied experimental data and predictions given by (16) is achieved for $\alpha = 83$.

The experimental data shows that the material grain size is reduced with the increase of the accumulated strain, asymptotically approaching the minimum achievable grain size (several hundred of nanometres). Theoretically the existence of minimum grain size can be explained by the fact that for smaller grain sizes, on the one hand, activation stresses for Frank–Read sources are beyond the flow stresses. On the other hand, dislocations are effectively dissolved by the grain boundaries. A critical stress for activation of Frank–Read sources is $\sigma_\tau = Gb/L_{FR}$,where $L_{FR} \sim 1/\sqrt{\rho_D} < d$ is a base of the Frank–Read source, proportional to inverse square root of the total dislocation density ρ_D. The maximum average stresses observed in the performed simulations after several ECAP passes are within the range of 350–400 MPa. Thus, $d_{\min} \sim 10/\sigma_\tau^{\max}$, which gives the experimentally observed grain sizes achievable by ECAP process. Smaller grain sizes are only achievable if an unstable plastic flow is developed. Possibly, this can be observed at a dynamic modification of ECAP process [27].

5. Conclusions

The comparison of the three models of dislocation density kinetics demonstrates that all of them are based on the classical model [6] and all give a good coincidence with the available experimental results [10,11]. In many cases the simplest classical model can be used in order to predict a defect hardening of the deformed material. Additional features for dislocation density based models given by separation of dislocations into mobile and immobile [7,9] or introduction of a law for evolution of cell wall volume fraction make the prediction of defect structure evolution more realistic, providing a possibility to account the changes in material fine structure.

2D modelling of a single ECAP pass of aluminium is performed for all the three discussed dislocation density based models. Distributions of dislocation densities within the sample are very similar for the models (1) and (4) with slight differences demonstrated by the model (6). The results received for the model [6] using parameters from [11] are very close to the results given by model [9] with the parameters taken from [10]. Despite the fact that the models based on dislocation density evolution are applicable and are in a good coincidence with the experimental measurements, a model for dynamic recrystallization coupling dislocation density with size of grain formed in the material is not sufficiently developed. Constant β used in this model is rather arbitrary and can obtain values between 3 (received by energetic reasoning) and 30 (received from condition of correspondence of predictions to the experimental data [10]). Due to this only inhomogeneity of defect distribution in material can be reliably predicted with numerical methods employing the existing approaches. In order to relate this distribution to absolute size of structure formed within the material, extensive additional experimental results are needed.

It is shown that if the Hall–Petch coefficient is known, a single numerical simulation of ECAP pass can be used in order to evaluate coefficient λ. Once λ is known, (13) can be used to receive the dependency of the grain size on the accumulated strain $d(\varepsilon)$ for any strain value. Thus, resultant grain size for arbitrary ECAP pass can be predicted.

In order to predict recrystallization for the whole range of grain sizes a new approach considering evolution of mobile and immobile dislocations is proposed. The received results are in a good coincidence with the available experimental data.

Among the advantages of this approach is the introduction of a single additional parameter (to be found from correspondence to experimental data) controlling DRX process instead of three fitting parameters introduced in another [23] known approach to the problem while the prediction accuracy is not reduced.

Acknowledgements

The research and publication preparation was supported by RFBR research grants 14-01-00814 and 13-01-00598, the President Grant for Government Support of Young Russian Scientists МД-286.2014.1, the Ministry of Education and Science of Russian Federation (scientific research of Chelyabinsk State University in the framework of competitive part of state assignment 3.1334.2014/K) and the academic programs of the Russian Academy of Sciences.

References

[1] V.M. Segal, Mater. Sci. Eng. A 271 (1999) 9322.
[2] R.Z. Valiev, R.K. Islamgaliev, I.V. Alexandrov, Prog. Mater. Sci. 45 (2000) 103–189.
[3] M.J. Zehetbauer, Y.T. Zhu (Eds.), Bulk Nanostructured Materials, Wiley-VCH Verlag GmbH & Co., KGaA, Weinheim, 2009.
[4] V.V. Popov, E.N. Popova, D.D. Kuznetsov, A.V. Stolbovsky, E.V. Shorohov, G. Reglitz, S.V. Divinski, G. Wilde, Mater. Sci. Eng. A 585 (2013) 281–291.
[5] I. Sabirov, M.Yu. Murashkin, R.Z. Valiev, Mater. Sci. Eng. A 560 (2013) 1–24.
[6] G.A. Malygin, Phys. Usp. 169 (1999) 979.
[7] A.E. Mayer, K.V. Khishchenko, P.R. Levashov, P.N. Mayer, Appl. Phys. J 113 (2013) 193508.
[8] A.E. Dudorov, A.E. Mayer, Vestn. Chelyabinsk State Univ. Phys. 39 (2011) 12.
[9] Y. Estrin, L.S. Toth, A. Molinari, Y. Brechet, Acta Mater. 46 (1998) 5509–5522.
[10] S.C. Baik, Mater. Sci. Eng. A 351 (2003) 86.
[11] J. Gubicza, Mater. Sci. Eng. A 387/389 (2004) 55.
[12] V.S. Krasnikov, A.E. Mayer, A.P. Yalovets, Int. J. Plast. 27 (2011) 1294–1308.
[13] C. Kittel, Introduction to Solid State Physics, Wiley & Sons, New York, 2005.
[14] D. McLean, Grain Boundaries in Metals, Clarendon Press, Oxford, 1957.
[15] A. Belyakov, T. Sakai, H. Miura, R. Kaibyshev, Philos. Magn. Lett. 80 (2000) 711–718.
[16] T. Sakai, A. Belyakov, R. Kaibyshev, H. Miura, J.J. Jonas, Prog. Mater. Sci. 60 (2014) 130–207.
[17] J. Gubicza, N.Q. Chinh, T.G. Langdon, T. Ungár, in: Y.T. Zhu, T.G. Langdon et.al. (Eds.), Ultrafine Grained Materials IV,2006.
[18] Y. Estrin, L.S. Tóth, Y. Bréchet, H.S. Kim, Mater. Sci. Forum 503 (2006) 675–680.
[19] M.A. Meyers, K.K. Chawla, Mechanical Behavior of Materials, Cambridge University Press, New York, 2009.
[20] J.P. Hirth, J. Lothe, Theory of Dislocations, Wiley & Sons, New York, 1982.
[21] M.A. Meyers, V.F. Nesterenko, J.C. LaSalvia, Y.B. Xu, Q. Xue, J. Phys. IV France 10 (2000) 51–56.
[22] D. Rittel, S. Osovski, Int. J. Fract. 162 (2010) 177–185.
[23] R. Lapovok, F.H. Dalla Torre, J. Sandlin, C.H.J. Davies, E.V. Pereloma, P.F. Thomson, Y. Estrin, J. Mech. Phys. Solids 53 (2005) 729–747.
[24] N. Lugo, J.M. Cabrera, N. Llorca, C.J. Luis, R. Luri, J. León, I. Puertas, Mater. Sci. Forum 584–586 (2008) 393–398.
[25] N.A. Enikeev, H.S. Kimb, I.V. Alexandrov, Mater. Sci. Eng. A 460–461 (2007) 619–623.
[26] R.W. Minich, C.A. Schuh, M. Kumar, Phys. Rev. B 66 (2002) 052101.
[27] E.N. Borodin, A.E. Mayer, Tech. Phys. 58 (2013) 1159–1163.